




Alternating phase focusing beam dynamics for drift tube linacs

Simon Lauber^{1*} , Winfried Barth^{1,2,3}, Markus Basten⁶, Florian D. Dziuba¹, Julian List^{1,2,3}, Maksym Miski-Oglu^{1,2}, Holger Podlech^{4,5} and Stepan Yaramyshev¹

*Correspondence: s.lauber@gsi.de

¹Linac Department, GSI
Helmholtzzentrum für
Schwerionenforschung, Darmstadt,
Germany
Full list of author information is
available at the end of the article

Abstract

In contrast to conventional E-mode resonance accelerators, H-mode DTLs provide for compact linac sections and have been established as highly efficient resonators during the last decades. Thus, H-mode structures are widely applied for heavy-ion acceleration with medium beam energies because of their outstanding capability to provide high acceleration gradients with relatively low energy consumption. To build upon those advantages, an alternating phase focusing beam dynamics layout has been applied to provide for a resonance accelerator design without internal lenses, which allows for eased commissioning, routine operation, maintenance, and potential future upgrades. The features of such a channel are going to be demonstrated on the example of two interdigital H-mode cavities, separated by an external quadrupole triplet. This setup provides for heavy ion (mass-to-charge ratio $A/z \leq 6$) acceleration from 300 keV/u to 1400 keV/u and is used as an injector part of the superconducting continuous wave accelerator HELIAC. Hence, this promising approach generally enables effective and compact routine operation for various applications, such as super heavy ion research, material science, and radio biological applications such as heavy-ion tumor therapy.

Keywords: Drift-tube linacs; Alternating phase focusing; Beam dynamics

1 Introduction

The GSI Helmholtzzentrum für Schwerionenforschung (GSI, Germany) is a leading research institution in the field of superheavy elements. Through the use of heavy ion beams provided by the Universal Linear Accelerator (UNILAC) [1–3], GSI has discovered six new heavy elements of the Mendeleev periodic table (elements 107 to 112) in the past few decades. However, the discovery of new superheavy elements has become more challenging due to the increased targeted mass of these synthesized elements, leading to a decrease in the probability of successful fusion. As a result, experiments now require weeks or even months [4] to conduct with the same linac. To address this challenge, an increase in the average beam current is necessary. For this purpose, either the current per bunch or the duty cycle of the delivering machine has to be increased. Since a high peak beam current is impractical to be delivered to the beam targets due to possible damage from heat, a high duty cycle is preferable. For continuous wave and high duty cycle applications of

© The Author(s) 2024. **Open Access** This article is licensed under a Creative Commons Attribution 4.0 International License, which permits use, sharing, adaptation, distribution and reproduction in any medium or format, as long as you give appropriate credit to the original author(s) and the source, provide a link to the Creative Commons licence, and indicate if changes were made. The images or other third party material in this article are included in the article's Creative Commons licence, unless indicated otherwise in a credit line to the material. If material is not included in the article's Creative Commons licence and your intended use is not permitted by statutory regulation or exceeds the permitted use, you will need to obtain permission directly from the copyright holder. To view a copy of this licence, visit <http://creativecommons.org/licenses/by/4.0/>.

heavy ion beams, superconducting machines have been proven to be more economical than their normal conducting counterparts [5].

Currently, the GSI main linac for heavy ion research UNILAC is upgraded [6–10] for beam delivery to the Facility for Antiproton and Ion Research (FAIR) SIS100 [11] synchrotron and its various experimental areas, as APPA [12], CBM [13], HADES [14], NUSTAR [15] and PANDA [16] among others (see Fig. 1). The new requirements for the beam are drastically different from the former demands, as the UNILAC will need to deliver a high peak-current beam at a low duty cycle. The new objectives of UNILAC operation are different from the before mentioned requirements for superheavy element research. Therefore, a new linear accelerator has been proposed to provide for energy variable, continuous wave heavy ion beam, dedicated to the discovery of new superheavy elements [17–19]. The Helmholtz Linear Accelerator (HELIAC) is going to deliver 1 mA average beam current of different ions from protons to uranium (see Table 1). The high average beam current will improve the time frame for measurement campaigns.

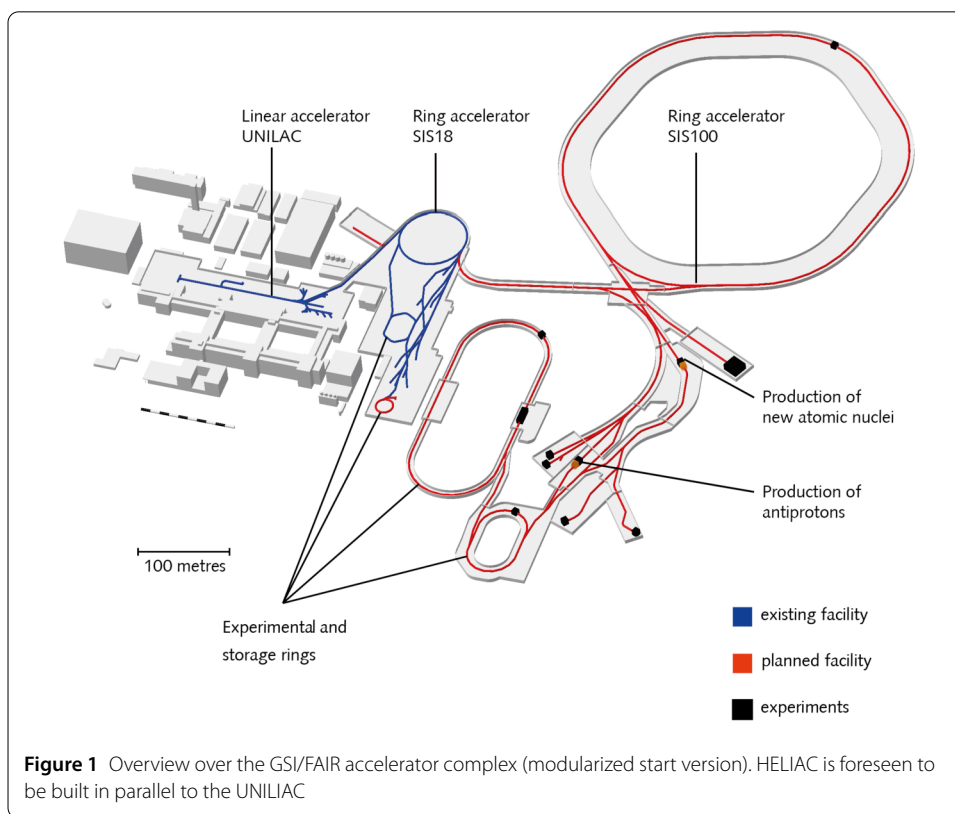


Table 1 Helmholtz Linear Accelerator specifications

Parameter	Value
Frequency	108.408 MHz
Mass-to-charge ratio A/z	1 to 6
Repetition rate	100%
Average beam current	1 mA
Output beam energy (variable)	3.5 MeV/u to 7.3 MeV/u
Cryomodules	4
Number of superconducting cavities	12

The Helmholtz Linear Accelerator was previously planned as a superconducting extension [18] to the already existing GSI High Charge State Injector (Hochladungsinjektor, HLI) [20]. Due to new planning directives in conjunction with the upgrade of the UNILAC, it has been decided to provide for a new dedicated injector, employing the HELIAC as an independent accelerator, nevertheless integrated into the GSI complex. Thus, a new design of the dedicated HELIAC injector has to be delivered. Following the bunch formation and pre-acceleration in the radio frequency quadrupole (RFQ), a normal conduction linac section is going to supply the beam to the superconducting main linac part. Two normal conduction interdigital H-mode (IH) cavities will provide for beam acceleration from 300 keV/u to 1400 keV/u beam energy [21].

It has been decided to adopt IH cavities, as crossbar H-mode cavities would be too compact longitudinally (at 216 MHz) or too big radially (at 108 MHz) for manufacturing, whereas Alvarez-type drift tube linacs (DTL) lack energy efficiency. Three approaches for the design of the normal conducting injector linac have been previously investigated, all based on IH cavities: designs with one, two, and three separate DTL cavities for heavy ion acceleration from 300 keV/u to 1400 keV/u. The layout with two cavities and an intermediate tank is preferred. A draft with three separately powered IH cavities was dismissed, as the two intertank sections in between the three cavities would have bloated the accelerator length. Furthermore, the operation of three radio frequency (RF) amplifiers and many quadrupole lenses could have aggravated the operation of such linac due to a high number of control parameters. The operation of one single IH cavity for the design specifications (see Table 1) is generally possible. The already existing HLI injector IH cavity employs a single resonator with embedded quadrupole lenses and is based on the Combined Zero Degree Structure (Kombinierte Null Grad Struktur, KONUS) beam dynamics concept, offering a space-efficient linac [22]. However, such a compact design results in the structure being sensitive to fluctuations of the control parameters during operation and does not feature the desirable beam diagnostics for eased operation. Furthermore, the installation and maintenance of quadrupole magnets embedded into the cavity demand a high budget.

Another approach to designing an efficient single DTL cavity is the application of alternating phase focusing (APF, see Sect. 2) beam dynamics. In this concept, internal magnetic lenses for transverse beam focusing are omitted inside the DTL cavity. Instead, positive synchronous phases are used to provide for the required transverse beam focusing. The mandatory longitudinal focusing is achieved with negative synchronous phases, traditionally used in the layout of linacs. In order to achieve beam focusing in all three room directions, positive and negative synchronous phases are used successively in an alternating sequence.

At the Heavy Ion Medical Accelerator facility (HIMAC, Japan), a single-cavity APF-linac is employed [23], partially comparable to our design specifications (cf. Table 1): a mass A to charge z ratio of $A/z = 3$, an injection energy of 400 keV/u and an output energy of 4 MeV/u of $^{12}\text{C}^{4+}$ carbon ions. The HIMAC APF structure's length is 3.4 m at a resonance frequency of 200 MHz and a duty cycle of 0.4%. The HIMAC APF linac proves the advantages of APF beam dynamics: the linac DTL is uncomplicated for operation, as the only control parameters are the cavity phase and voltage. Therefore, it is highly suited as a medical injector due to rapid recommissioning periods. Furthermore, it has been reported that the operation of APF linacs, in general, can reduce construction and operation costs by about 30% [24].

In comparison to HIMAC, for HELIAC the transported mass-to-charge ratio is twice as high [21]. Preliminary investigations of a single-cavity APF acceleration system (see Sect. 4.1) for the HELIAC injector indicated high-quality beam transport with up to 90% of the design emittance, but no satisfying solution has yet been found for the 10% higher design emittance. Also, obtaining high beam quality with such high beam emittance requires strict fabrication tolerances. Thus, for the HELIAC injector, it has been decided to adopt a linac design using two APF cavities (see Sect. 4.2), separated by an intertank equipped with a quadrupole triplet for extra transverse beam focusing. The hybrid approach combines the advantages of highly adjustable quadrupole focusing with the low number of control parameters from the APF concept and reduced construction costs. The intertank also allows the installation of transport and diagnostic equipment, that could not have been installed in a single-cavity machine. In particular, the additional quadrupole triplet is mandatory to cope with varying beam parameters, which could be encountered during operation of the electron cyclotron resonance ion source with very different ion species, as required for material and superheavy ion research.

Due to the high effort of making a production ready cavity design, only the separate cavity design has been finalized. Nevertheless, both the preliminary single-cavity APF design and the final separate cavity APF design are presented in this publication to provide insight into critical design decisions for APF accelerators.

2 Alternating phase focusing

The principle of Alternating Phase Focusing (APF) was first proposed independently by J. Adlam [25] and M. Good [26] in 1953, and also in the Soviet Union by I. Fainberg in 1956 [27]. The theoretical framework for APF was consequently elaborated further by I. M. Kapchinsky [28] in the years after. However, it was not until 2007 that the actual operation of an APF linac was reported by Y. Iwata et al. [29]. Despite its early development, the APF beam dynamics principle was not widely used due to the limited computer power available for design at the time. This was due to the challenging nature of the beam dynamics calculation and the difficulty in predicting the properties of the resulting RF structures. With the current state of software technology, these challenges are no longer a barrier.

APF cavities have no magnetic lenses inside them. To avoid using magnetic focusing elements, the electric field of the RF gaps is used to accelerate and also to focus the beam. However, Gauss's law, a fundamental Maxwell equation, states that it's not possible to focus the beam simultaneously in all directions in charge-free space, $\nabla \cdot \vec{E} = 0$. Thus, sequential longitudinal and transverse electric focusing is necessary to provide for overall beam focusing. Positive and negative synchronous phases (i.e., the RF phase when the accelerated particle beam passes the RF gap) are applied alternately to provide for the transversal and longitudinal focusing. Negative phases are routinely applied for acceleration and longitudinal focusing, whereas positive phases for transverse focusing have found wider application during recent decades, although proposed already in 1953 and refined in following years. Since then, computational power has increased by several orders, as predicted by Moore's Law [30]. Recently, it is possible to provide a design and detailed analysis of the complex beam transport in alternating phase focusing accelerators. From a beam dynamics point of view, the core task in APF cavity design is selecting the synchronous phases ϕ_i for each gap to obtain the preferred accelerating/focusing properties. The gradual change from negative to positive synchronous phases is realized by altering the $\beta\lambda/2$

resonance acceleration geometry of a cavity. The introduced synchronous phase change $\Delta\phi$ in between two neighboring RF gaps leads to a change of the resonator geometry: the lengths of the tubes inside the DTL cavity are decreased/increased:

$$L_{\text{cell}} = \frac{\beta\lambda}{2} + \beta\lambda \frac{\Delta\phi}{360^\circ} \quad (1)$$

The changed cell length affects the time a particle bunch needs to travel from one RF gap to another. The altered arrival timing of the bunch in the next gap thus leads to a changed synchronous phase.

To achieve full beam transmission and a high beam quality in an APF linac, the designer must choose the synchronous phase for each gap individually. This also allows more flexibility during RF design, as the voltage profile along the cavity is not constrained by beam dynamics to be very flat. It requires several iterations to converge the voltage profile of the RF design and the synchronous phase profile from beam dynamics to a consistent geometry, as they are mutually dependent.

However, design and fabrication of the DTL geometry becomes more demanding due to the tight tolerance condition (of about 2%) between the voltage used in the beam dynamics and the actual voltage in the cavity [31]. In particular, this dedicated tolerance has to be considered during design of the dynamic frequency tuning concept, as the moving parts used for tuning crucially interfere with the electromagnetic field.

3 Methods

3.1 Beam transport model

In general, the energy gain of a particle with charge $q = z \cdot e$ depends on the voltage U_0 in an RF gap, the transit time factor T_{TTF} and the synchronous phase ϕ [32].

$$\Delta W = qU_0 T_{\text{TTF}} \cos(\phi) \quad (2)$$

Furthermore, the transverse focusing strength $k_{(x,y)}$ depends on the mass m_0 , velocity v , the Lorentz factor γ and the RF wavelength λ [32]

$$k_{(x,y)} = -1 \frac{\pi q U_0 T_{\text{TTF}}}{m_0 v^2 \gamma^2 \lambda} \sin(\phi) \quad (3)$$

The longitudinal focusing strength k_z , is twice as strong [32]:

$$k_z = 2 \frac{\pi q U_0 T_{\text{TTF}}}{m_0 c^2 \beta^2 \lambda} \sin(\phi) \quad (4)$$

Thus, the focusing properties in all three room-dimensions $u \in \{x, y, z\}$ could be calculated by means of matrix multiplication of the particle coordinates x in mm and relative velocities x' in mrad with the transport matrix M [32].

$$M_u \vec{x}_u = \begin{pmatrix} 1 & 0 \\ k_u / (\beta\gamma)_f & (\beta\gamma)_i / (\beta\gamma)_f \end{pmatrix} \cdot \begin{pmatrix} x_u \\ x'_u \end{pmatrix} \quad (5)$$

For accurate calculation of the beam transport, the volumetric transit time factor could be used, considering the radial position of the particle r , the aperture radius a , and the gap

length g [33, pp. 33].

$$T_{\text{TF}}(r) = I_0(Kr) \frac{J_0(2\pi a/\lambda) \sin(\pi g/(\beta\lambda))}{I_0(Ka) \pi g/(\beta\lambda)} \quad (6)$$

The constant K scales reciprocal with the particle velocity $K = 2\pi/(\gamma\beta\lambda)$. The Bessel and modified Bessel functions are denoted as $I_0(x)$ and $J_0(x)$.

Equation (5) is routinely used for efficient calculations of beam dynamics transport because of its vectorized format, by assigning the average phase ϕ_{ref} and a common transit time factor to all particles. But the mathematical averaging to achieve maximum software performance is not expedient for the calculation of the beam dynamics in an APF channel. To cover the features of the overall non-linear beam transport, the tracking must be accurately conducted for each individual particle to account for the coupling of particle phase to transverse focusing, as well as to accurately reflect the term $\sin(\phi_i)$ of each particle. Either, the above equations are implemented for tracking of individual particles separately, or already existing modern particle tracking software could be employed.

Nevertheless, the particle tracking from one RF gap to the next could be implemented efficiently by using the drift matrix D and the cell length according to Equation (1) [32].

$$D_u \vec{x}'_u = \begin{pmatrix} 1 & L_{\text{cell}}/K_u \\ 0 & 1 \end{pmatrix} \cdot \begin{pmatrix} x_u \\ x'_u \end{pmatrix} \quad (7)$$

The constant K_u equals $K_{x,y} = 1$ transversely and to $K_z = \gamma^2$ longitudinally. The transport through the APF linac is calculated iteratively by updating the particle coordinates $x_{u,i}$ and relative velocities $x'_{u,i}$, as well as the beam energy $E_{\text{kin},i}$ for each gap i directly by applying Equation (1), (2), (5), and (7).

3.2 Input beam distribution

An input particle distribution must be selected as a starting point for particle tracking. To analyze the beam dynamics with the lowest number of particles, it is proposed to solely cover the border of the 6D phase space, whilst the inner positions within the hypersphere could be transported with even higher beam quality. To obtain a 6D hypersphere, a multivariate normal distribution must be rescaled according to the 6D Twiss equation [34]

$$\frac{\widehat{\gamma}_x x^2 + 2\widehat{\alpha}_x x x' + \widehat{\beta}_x x'^2}{\widehat{\epsilon}_x} + \frac{\widehat{\gamma}_y y^2 + 2\widehat{\alpha}_y y y' + \widehat{\beta}_y y'^2}{\widehat{\epsilon}_y} + \frac{\widehat{\gamma}_z z^2 + 2\widehat{\alpha}_z z z' + \widehat{\beta}_z z'^2}{\widehat{\epsilon}_z} = 1, \quad (8)$$

using the Twiss parameters $\widehat{\alpha}_u$, $\widehat{\beta}_u$, $\widehat{\gamma}_u$ and $\widehat{\epsilon}_u$. The presented distribution has a total-to-RMS emittance ratio of 6 and therefore corresponds to a Waterbag distribution.

3.3 Determination of the synchronous phases along the drift tube linac

The beam focusing and acceleration within the cavity should be designed to obtain maximum acceleration efficiency with minimum emittance growth. To obtain an appropriate solution, the input Twiss parameters $\widehat{\alpha}_u$, $\widehat{\beta}_u$, and $\widehat{\gamma}_u$, as well as the synchronous phase ϕ_i in each gap must be selected correspondingly. For identification of the optimum variables, several numeric global and local optimization strategies are available [35].

Amongst the vast amount of algorithms that are available, Nelder-Mead [35, 36], Differential Evolution [35, 37] and Random Search method (outlined in [21]) were applied.

Table 2 Limitations of the Twiss parameters to produce the discussed cavities by optimization

Variable	Min	Max
$\alpha_{\text{transversal}}$	-2	2
$\beta_{\text{transversal}}$	0.1 mrad/mm	2 mrad/mm
$\alpha_{\text{longitudinal}}$	-1	1
$\beta_{\text{longitudinal}}$	1 KeV/u/deg	4 KeV/u/deg

The Random Search algorithm was applied to find the solution for the separate cavity setup. With the gained experience in optimization of APF cavities, it was decided later to use global (Differential Evolution) and local optimization (Nelder-Mead) to produce the presented single cavity design.

A key aspect of the optimization of the variables is the adoption of an objective function, translating the designer's requirements into a formal measure. The implemented objective function is detailed in [21] and targets minimum emittance growth ξ_u , as well as a high output energy W_{out} .

$$f = \left(\frac{\xi_{x,y} - 1}{t_{x,y}} \right)^2 + \left(\frac{\xi_z - 1}{t_z} \right)^2 + \frac{W_{\text{target}} - W_{\text{out}}}{t_E} \quad (9)$$

The terms of the objective functions are designed to yield a value between 0 and 1 if the variables are below their corresponding target tolerance t , otherwise, the result is a value greater than 1. The target energy is intentionally left without exponent to allow for even higher output energy than the targeted, provided that the emittance growth does not increase dramatically.

The variables of the optimization, i.e., the input Twiss parameters $\hat{\alpha}_u$, $\hat{\beta}_u$, and $\hat{\gamma}_u$, and the synchronous phase ϕ_i in each gap, are constrained. Extreme combinations of Twiss parameters are not desired, as the actual transport systems might not be able to deliver them (the specific numbers of these limits depend on the scope of the design, e.g., mass to charge ratio, emittance, aperture). The paper specific bounds are listed in Table 2.

The phases in all gaps are at least constrained by the physical length of the drift tubes, as too short cells from rapid changes in the synchronous phase could cause too narrow cell lengths. From an RF point of view, also too long tubes could be impractical due to heat overload. Therefore, in addition to a $+90^\circ$ to -90° , also the resulting tube/gap geometry must be regarded and constrained for optimization. For the presented results, the tube and gap length was forced to be bigger $\beta\lambda/8$ and smaller $\beta\lambda$.

4 Results

In this section, the results of a preliminary single cavity design are discussed (see Sect. 4.1), as well as the final design of the HELIAC APF injector linac with two separate cavities (see Sect. 4.2). Both designs were obtained using a specifically previously developed optimization function, wrapping the multi-particle tracking code DYNAMION [38]. In order to put the results in perspective, Table 3 outlines the results of the presented and similar APF channels from other authors. Table 4 displays the used phases to obtain the results below.

4.1 Single cavity with alternating phase focusing

A feasibility study was conducted in order to determine, if a single cavity applying APF beam dynamics could be realized with the required input emittance. The cavity was opti-

Table 3 Overview on APF linacs worldwide

	HIMAC Medical Syn- chrotron injector [23, 29]	J-PARC Muon Linac [39–42]	325 MHz Proton medical injector [43–45]	HELIAC injector – two cavities [21, 46]	Compact IH [47–49]	HELIAC injector – single cavity layout	Medical Syn- chrotron injector [24]
Status of realization	in operation	com-mis-sioned with beam	com-mis-sioned with beam	in fabri-cation	high-power test	designed	designed
Mass-to-charge ratio A/z	3	0.1	1	6	1	6	3
Input energy (keV/u)	608	3000	3000	300	220	300	300
Output energy (keV/u)	4000	40000	7000	1400	2000	1400	7000
Max. gap voltage (kV)	350	NA	250	260	180	180	450
Length (m)	3.4	1.3	1.5	4.5 (3) ^a	1.5	3.4	4.3
Frequency (MHz)	200	324	325	108	100	108	216
Duty factor (%)	0.4	0.1	0.005–0.01	100	NA	NA	NA
Number of cells	72	16	32	29 + 27	22	60	78
Aperture radius (mm)	7	5 to 9	6	9	NA	10	12; 16
Kilpatrick factor	1.6	1.8	1.53	2.5	NA	NA	NA
Transmission (%)	99.6	98	98 (68) ^b	100	80	100	100
Energy gain (MeV)	10.176	3.7	4	6.6	1.96	6.6	20.1
Effective gradient (MV/m)	3	2.8	2.6	1.5	1.3	2	4.7
Norm. transv. 90% input emit. (mm mrad)	0.68	NA	NA (< 1.0)	0.4	NA (1 acceptance)	0.4	0.32
Transv. emit. growth (%)	25	NA	NA	5	NA	12	70
Long. 90% input emit. (keV ns/u)	1.3	NA	NA (< 6)	1.64	NA (0.08 acceptance)	1.64	0.88
Long. emit. growth (%)	23	NA	NA	3	NA	10	11

^a3 m without intertank section.

^b“effective transmission” [44].

mized for beam transport with a transverse normalized input emittance of 0.8 mm mrad and 1.64 keV ns/u longitudinally (foreseen by to be delivered by the preceding RFQ), and a field gradient of 3 MV/m for acceleration from 300 keV/u to 1400 keV/u. The transverse envelopes are limited by the aperture of 10 mm.

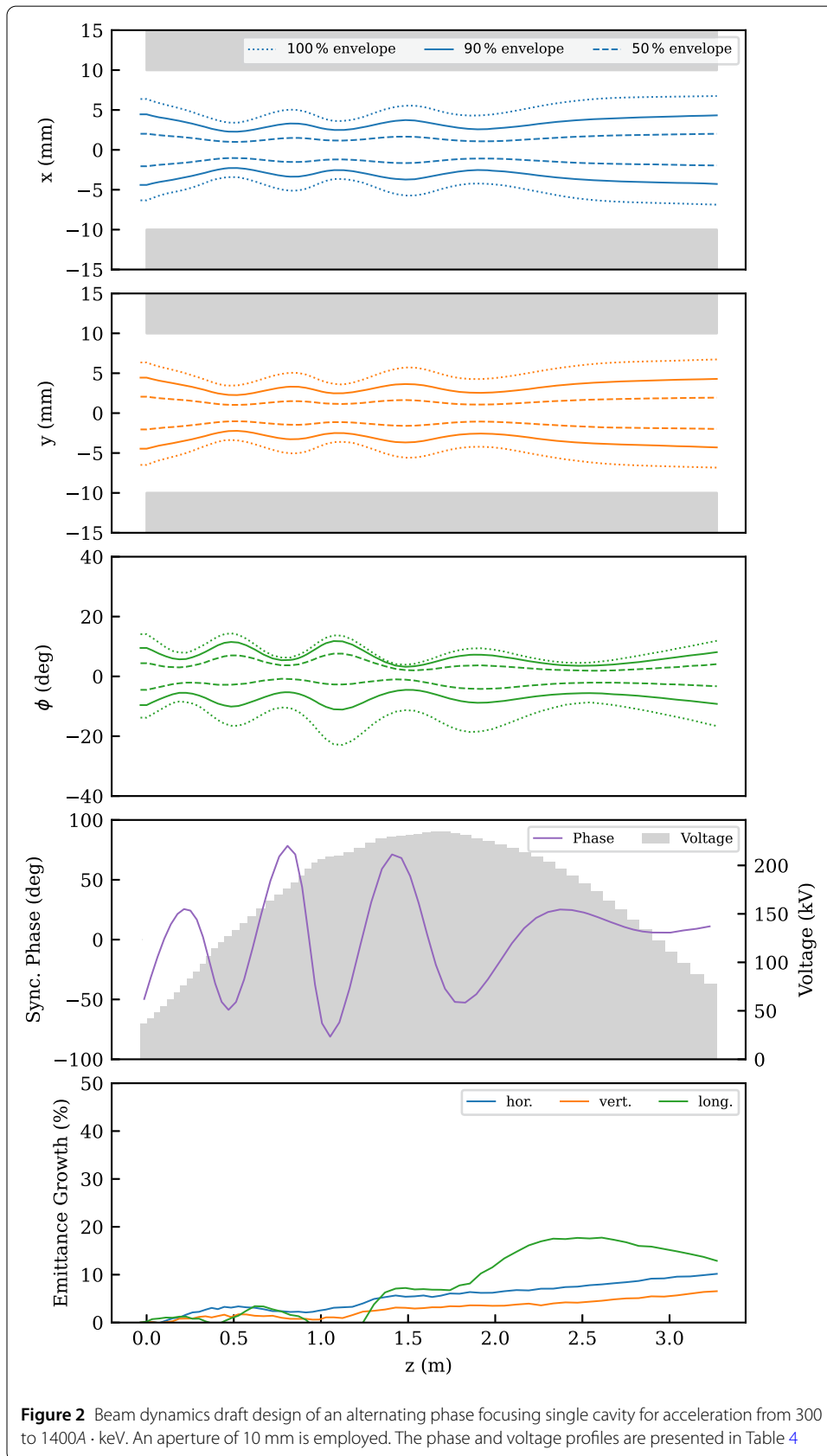
With the electric field gradient $E_0 = 3 \text{ MV/m}$, $T_{\text{TF}} \approx 0.8$, the energy gain $\Delta W = 1.4 \text{ MeV/u} - 0.3 \text{ MeV/u}$, the average phase equivalent $0.8 = \sin(\phi_{\text{avg}} \approx 35^\circ)$, and a mass to charge ratio of 6, one can estimate the accelerator length of 3.4 m.

The set of synchronous gap phases along the cavity were obtained using the matrix-method for beam propagation and the SciPy differential evolution algorithm [35, 37]. After obtaining the set of synchronous phases, the cavity beam dynamics was then again modeled using DYNAMION to confirm the results of the matrix solver.

Hence, the resulting trajectories from DYNAMION after optimization are depicted in Fig. 2. No particle loss occurs within the 3.4 m long structure, whereas the 100%-transverse envelope is close to the aperture and the 90%-envelope size is smaller than half of the aperture along the DTL cavity. The longitudinal 100%-envelope is asymmetric,

Table 4 Voltages and phases in each gap of the two presented linac options

Gap Nr.	Two cavities [21]		Single cavity	
	Phase (deg)	Voltage (kV)	Phase (deg)	Voltage (kV)
1	-53.5	46.7	-49.6	37.15
2	-47.9	97.6	-31.4	42.02
3	-33.3	108.4	-14.4	48.41
4	-13.9	118.6	0.6	54.99
5	6.5	128.0	12.8	61.76
6	24.2	136.8	21.4	68.67
7	39.5	144.6	25.5	75.93
8	50.8	151.4	24.3	83.09
9	47.9	156.3	16.8	90.74
10	27.4	160.4	2.4	98.71
11	-0.2	163.3	-16.8	106.54
12	-31.6	165.6	-36.4	114.25
13	-66.0	166.8	-51.8	121.04
14	-84.0	167.8	-58.4	127.34
15	-78.1	168.4	-51.9	133.35
16	-22.5	167.5	-33.2	140.02
17	27.5	165.5	-6.9	147.37
18	50.5	163.2	22.1	155.35
19	59.7	160.4	49.2	163.28
20	55.8	158.2	69.5	170.32
21	42.8	154.3	78.5	176.40
22	22.9	148.2	71.1	182.54
23	0.5	143.0	44.1	189.13
24	-22.8	136.7	4.1	196.32
25	-47.6	129.5	-37.5	202.87
26	-59.4	120.6	-69.6	206.70
27	-62.3	110.1	-80.9	208.96
28	-58.1	97.8	-68.8	210.49
29	-51.1	46.4	-40.8	213.24
30	-77.7	62.5	-4.7	217.71
31	-100.6	132.7	31.2	223.09
32	-106.9	151.1	59.1	227.47
33	-84.4	173.3	71.6	229.78
34	9.2	196.5	68.2	230.64
35	43.7	214.7	53.0	231.38
36	35.6	228.2	30.3	232.36
37	24.9	239.6	4.2	233.79
38	12.6	249.7	-20.9	235.01
39	3.7	257.6	-41.1	235.13
40	-2.5	263.8	-52.1	233.68
41	-8.5	267.8	-52.8	231.39
42	-14.3	268.8	-45.7	228.34
43	-17.7	2687	-33.3	225.14
44	-17.4	265.6	-18.2	221.83
45	-15.4	260.8	-3.1	218.22
46	-13.4	253.8	9.3	214.06
47	-9.0	244.8	17.9	209.13
48	-3.9	233.7	22.9	203.39
49	2.3	221.2	24.9	196.85
50	9.4	206.6	24.6	189.58
51	15.6	189.5	22.5	181.64
52	21.0	171.9	19.2	173.13
53	27.2	153.2	15.4	164.06
54	33.6	133.1	11.6	154.46
55	40.1	111.9	8.4	144.36
56	45.9	51.5	6.4	133.78
57		1.2	5.7	122.78
58		4.5	6.1	111.38
59		11.4	7.4	99.67
60		23.5	9.2	87.68



whereas the 90%-envelope is almost symmetrical. This observation is also reflected by the emittance growth metric. The 90%-effective emittance growth is about 10% transversely and 12% longitudinally. Those figures of merit are superb, but the total emittance growth and consequently the beam size and potential losses render this result unpreferable for application in a continuous wave linear accelerator, as even a few percent particle loss along decades of actual operation could impose degradation of the machine performance.

The model of this single cavity with alternating phase focusing was obtained in about two weeks of work and does not reflect a final optimum solution, but rather an intermediate one, as it was decided early to design an APF channel using two separate cavities to allow a highly flexible robust routine operation, also necessary to compensate varying beam conditions from the operation of the ion source with very different ion species. As discussed in the following section, this cavity would have been analogously bordered by two transport sections, equipped with rebunchers and quadrupoles to match the beam of the RFQ to the required input parameter and to the superconducting main accelerator.

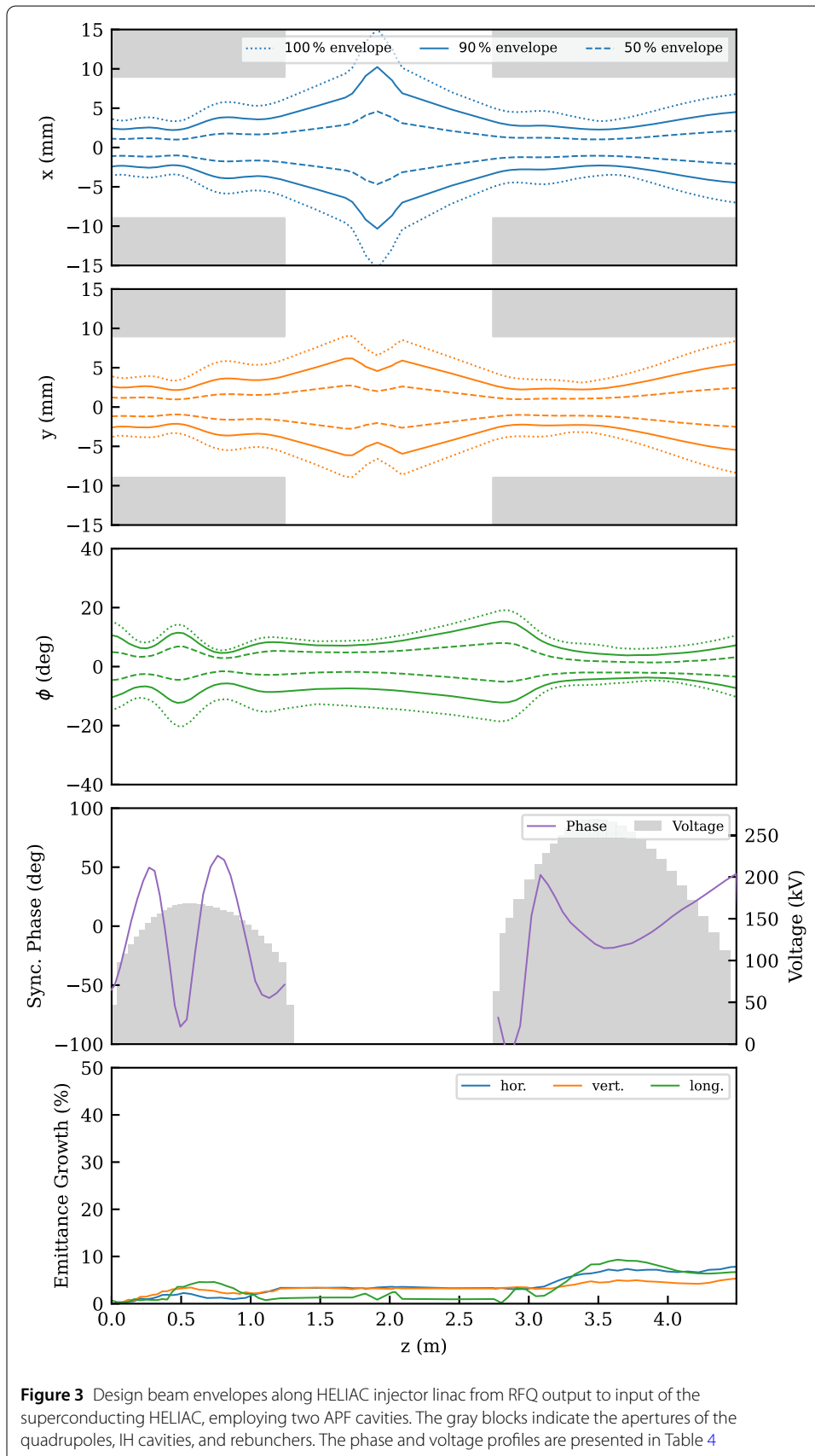
4.2 Two separate cavities with alternating phase focusing

The second variant to design an APF channel (see Fig. 3) for continuous wave application was realized by employing two separate IH cavities (Cavity-1 & 2) with a quadrupole triplet in between them (Intertank). A detailed report on the channel design is published in [21], thermal and RF considerations are published in [46]. The cavities were individually designed employing DYNAMION and Random Search.

As already mentioned, the intertank triplet is used to compensate beam parameters different from the reference design. Also, beam diagnostics as phase probe sensors and beam position monitors will be installed in the channel in the intertank region. The additional beam diagnostics will provide for easy commissioning, as well as routine operation.

The channel was designed employing a field gradient of 3 MV/m and an aperture radius of 9 mm for the acceleration of a beam with a transverse normalized emittance of 0.8 mm mrad and 1.64 keV ns/u longitudinally (the same as for option 1). For integration into the HELIAC injector, the corresponding beam transport lines have been designed as well. The Medium Energy Beam Transport system is equipped with a quadrupole doublet and a triplet, as well as a rebuncher for longitudinal beam matching to the acceptance of the first cavity.

Cavity-1 (until 1.3 m in Fig. 3) accelerates the beam to an intermediate energy of 700 keV/u. The quadrupole triplet in the intertank (1.3 m to 2.8 m) refocuses the transversely divergent beam. A rebuncher is not installed to the intertank, as Cavity-1 provides dedicated output parameters to match the beam longitudinally to Cavity-2. The beam is accelerated to the final energy of 1400 keV/u along Cavity-2. Due to the preceding transverse beam focusing, the synchronous phase pattern in Cavity-2 is oriented rather to beam acceleration than to transverse focusing. The final matching section (> 6.1 m) is equipped with two quadrupole doublets and two rebuncher cavities for full 6D matching of the beam to the acceptance of the superconducting HELIAC. The 90%-effective emittance growth of the channel is about 5% transversely and 3% longitudinally, and thus suited to supply high-quality beam to the superconducting HELIAC and subsequent experiments.



5 Conclusion

Alternating phase focusing (APF) cavities are an appealing option for extending the length of drift tube linacs (DTL) without the need for embedded magnetic lenses, resulting in a compact design, effective acceleration, and a relatively low price tag. The magnet-free design makes fabrication easier and the reduced number of control parameters contributes to a smooth commissioning process, as well as stable operation. Two implementations of the APF beam dynamics scheme for $\beta\lambda/2$ drift tube linacs have been elaborated for the acceleration of heavy ions from 300 keV/u to 1400 keV/u: a single DTL without any magnetic lens, and a channel with two APF cavities separated by an intertank, equipped with an external quadrupole triplet. The first option provides for a 90%-effective emittance growth of about only 10% longitudinally, but 12% transversely. Potential losses due to the total beam size make this option unsuitable for continuous wave operation with 1 mA beam current. This preliminary design holds potential for applications that involve a lower average beam current, owing to its compactness, effectiveness, and limited number of control parameters (i.e., tank phase and voltage). However, further improvements can be made to enhance its performance. The second option, which utilizes two separate APF cavities and external quadrupole focusing, has been extensively developed and demonstrates high beam quality (with only 4% transverse and 3% longitudinal 90%-emittance growth) making it the preferred acceleration unit for the injector of the superconducting Helmholtz Linear Accelerator.

Acknowledgements

The publication is funded by the Deutsche Forschungsgemeinschaft (DFG, German Research Foundation) – 491382106, and by the Open Access Publishing Fund of GSI Helmholtzzentrum für Schwerionenforschung. Furthermore, we gratefully acknowledge the support provided by the HBS Innovation Pool project of the Research Field Matter of the Helmholtz Association. In addition, we thank Christina Will of the GSI Mechanical Integration group for technical support in the design and implementation of the layout of the two APF-IH cavities.

Funding

Open Access funding enabled and organized by Projekt DEAL. This work is supported by the HBS Innovation Pool Project of the Research Field Matter of the Helmholtz Association.

Abbreviations

GSI, GSI Helmholtzzentrum für Schwerionenforschung; UNILAC, Universal Linear Accelerator; FAIR, Facility for Antiproton and Ion Research; HELIAC, Helmholtz Linear Accelerator; HLI, Hochladungsinjektor; RFQ, radio frequency quadrupole; IH, interdigital H-mode; DTL, drift tube linac; RF, radio frequency; KONUS, Kombinierte Null Grad Struktur; APF, alternating phase focusing; HIMAC, Heavy Ion Medical Accelerator.

Data availability

The datasets used and/or analysed during the current study are available from the corresponding author on reasonable request.

Declarations

Competing interests

The authors declare that they have no competing interests.

Author contributions

All authors read and approved the final manuscript.

Author details

¹Linac Department, GSI Helmholtzzentrum für Schwerionenforschung, Darmstadt, Germany. ²Accelerator Design and Integrated Detectors, Helmholtz Institut Mainz, Mainz, Germany. ³Institut für Kernphysik, Johannes Gutenberg-Universität, Mainz, Germany. ⁴Institut für Angewandte Physik, Goethe-Universität, Frankfurt am Main, Germany. ⁵Helmholtz Research Academy Hesse for FAIR Campus Frankfurt, GSI Helmholtz Centre for Heavy Ion Research, Darmstadt, Germany. ⁶Carl Zeiss SMT GmbH, Roßdorf, Germany.

References

1. Barth W, Hollinger R, Adonin A, Miski-Oglu M, Scheeler U et al. LINAC developments for heavy ion operation at GSI and FAIR. *J Instrum.* 2020;15(12):12012. <https://doi.org/10.1088/1748-0221/15/12/t12012>.
2. Barth W, Scheeler U, Vormann H, Miski-Oglu M, Vossberg M et al. High brilliance beam investigations at the universal linear accelerator. *Phys Rev Accel Beams.* 2022;25:040101. <https://doi.org/10.1103/PhysRevAccelBeams.25.040101>.
3. Vormann H, Barth W, Miski-Oglu M, Scheeler U, Vossberg M et al. High current heavy ion beam investigations at GSI-UNILAC. *J Phys Conf Ser.* 2023;2420(1):012037. <https://doi.org/10.1088/1742-6596/2420/1/012037>.
4. Khuyagbaatar J, Yakushev A, Düllmann CE, Ackermann D, Andersson LL et al. Search for elements 119 and 120. *Phys Rev C.* 2020;102(6):064602. <https://doi.org/10.1103/PhysRevC.102.064602>.
5. Podlech H. Superconducting versus normal conducting cavities. Technical Report CERN-2013-001.151, CERN. 2013. [arXiv:1303.6552](https://arxiv.org/abs/1303.6552). <https://doi.org/10.5170/CERN-2013-001.151>.
6. Barth W, Bayer W, Dahl L, Groening L, Richter S et al. Upgrade program of the high current heavy ion UNILAC as an injector for FAIR. *Nucl Instrum Methods Phys Res, Sect A.* 2007;577(1):211–4. <https://doi.org/10.1016/j.nima.2007.02.054>.
7. Barth W, Adonin A, Düllmann CE, Heilmann M, Hollinger R et al. U^{28+} -Intensity record applying a H_2 -gas stripper cell. *Phys Rev Spec Top, Accel Beams.* 2015;18(4):040101. <https://doi.org/10.1103/PhysRevSTAB.18.040101>.
8. Adonin A, Barth W, Heymach F, Hollinger R, Vormann H et al. Production of high current Proton beams using complex H-rich molecules at GSI. *Rev Sci Instrum.* 2016;87:02. <https://doi.org/10.1063/1.4934620>.
9. Barth W, Adonin A, Appel S, Gerhard P, Heilmann M et al. Heavy ion linac as a high current Proton beam injector. *Phys Rev Spec Top, Accel Beams.* 2015;18:050102. <https://doi.org/10.1103/PhysRevSTAB.18.050102>.
10. Yaramyshev S, Vormann H, Adonin A, Barth W, Dahl L, et al. Virtual charge state separator as an advanced tool coupling measurements and simulations. *Phys Rev Spec Top, Accel Beams.* 2015;18. <https://doi.org/10.1103/PhysRevSTAB.18.050103>.
11. Spiller P, Bals R, Bartolome P, Blaurock J, Blell U et al. The FAIR heavy ion synchrotron SIS100. *J Instrum.* 2020;15(12):12013. <https://doi.org/10.1088/1748-0221/15/12/t12013>.
12. Stöhlker T, Bagnoud V, Blaum K, Blazevic A, Bräuning-Demian A, et al. APPA at FAIR: from fundamental to applied research. *Nucl Instrum Methods Phys Res B.* 2015;365. <https://doi.org/10.1016/j.nimb.2015.07.077>.
13. Herrmann N. Status and perspectives of the CBM experiment at FAIR. *EPJ Web Conf.* 2022;259:09001. <https://doi.org/10.1051/epjconf/202225909001>.
14. Lapidus K, Gumberidze M, Hennino T, Rosier P, Ramstein B. The HADES-at-FAIR project. 2012.
15. Nilsson T. The NUSTAR project at FAIR. *Phys Scr T.* 2015;166:014070. <https://doi.org/10.1088/0031-8949/2015/T166/014070>.
16. Schmidt M. The panda detector at fair. *Ukr J Phys.* 2019;64:640. <https://doi.org/10.15407/ujpe64.7.640>.
17. Minaev S, Ratzinger U, Podlech H, Busch M, Barth W. Superconducting, energy variable heavy ion linac with constant β , multicell cavities of CH-type. *Phys Rev Spec Top, Accel Beams.* 2009;12:120101. <https://doi.org/10.1103/PhysRevSTAB.12.120101>.
18. Schwarz M, Yaramyshev S, Aulenbacher K, Barth W, Basten M, et al. Reference beam dynamics layout for the SC CW heavy ion HELIAC at GSI. *Nucl Instrum Methods Phys Res, Sect A.* 2019;163044. <https://doi.org/10.1016/j.nima.2019.163044>.
19. Barth W, Aulenbacher K, Basten M, Dziuba F, Gettmann V et al. A superconducting CW-linac for heavy ion acceleration at GSIX. *EPJ Web Conf.* 2017;138:01026. <https://doi.org/10.1051/epjconf/201713801026>.
20. Klabunde J. The high charge state injector for GSI. In: *Proc. LINAC'92.* 1992. p. 570–4.
21. Lauber S, Yaramyshev S, Basten M, Aulenbacher K, Barth W et al. An alternating phase focusing injector for heavy ion acceleration. *Nucl Instrum Methods Phys Res, Sect A.* 2022;1040:167099. <https://doi.org/10.1016/j.nima.2022.167099>.
22. Ratzinger U, Hähnel H, Tiede R, Kaiser J, Almomani A. Combined zero degree structure beam dynamics and applications. *Phys Rev Accel Beams.* 2019;22(11):114801. <https://doi.org/10.1103/PhysRevAccelBeams.22.114801>.
23. Iwata Y, Yamada S, Murakami T, Fujimoto T, Fujisawa T et al. Alternating-phase-focused IH-DTL for an injector of heavy-ion medical accelerators. *Nucl Instrum Methods Phys Res, Sect A.* 2006;569(3):685–96. <https://doi.org/10.1016/j.nima.2006.09.057>.
24. Minaev S, Ratzinger U, Schlitt B. APF or KONUS drift tube structures for medical synchrotron injectors—a comparison. In: *Proc. PAC'99.* vol. 5. 1999. p. 3555–7. <https://doi.org/10.1109/PAC.1999.792368>.
25. Adlam JH. A method of simultaneously focusing and accelerating a beam of Protons. *AERE GP/M.* 1953;146.
26. Good ML. Phase-reversal focusing in linear accelerators. *Phys Rev.* 1953;92:538. Berkeley Radiation Laboratory report.
27. Fainberg IB. Alternating phase focusing. In: *Proc. Conf. on high energy accelerators.* Geneva: CERN; 1956. <https://doi.org/10.5170/CERN-1956-025.91>.
28. Kapchinskiy IM. *Theory of linear resonance accelerators.* Reading: Harwood Academic; 1985.
29. Iwata Y, Yamada S, Murakami T, Fujimoto T, Fujisawa T et al. Performance of a compact injector for heavy-ion medical accelerators. *Nucl Instrum Methods Phys Res, Sect A.* 2007;572(3):1007–21. <https://doi.org/10.1016/j.nima.2007.01.012>.
30. Moore GE. Cramming more components onto integrated circuits. *Electronics.* 1965;38(8).
31. Kapin V, Iwata Y, Yamada S. Effects of field distortions in IH-APF linac. *Proc RuPAC.* 2004. 459–461.
32. Crandall RK, Rusthoi PD. TRACE-3D User's manual. Technical Report LA-UR-97-886. Los Alamos National Laboratory; 1997.
33. Wangler TP. *RF linear accelerators.* New York: Wiley; 2008. <https://doi.org/10.1002/9783527623426.fmatter>.
34. Shor A, Feinberg G, Halfon S, Berkovits D. SARAF simulations with 6D waterbag and gaussian distributions. Technical Report INIS-IL-011. Soreq NRC, Israel; 2004. http://inis.iaea.org/search/search.aspx?orig_q=RN:35095272.
35. Virtanen P, Gommers R, Oliphant TE, Haberland M, Reddy T et al. SciPy 1.0: fundamental algorithms for scientific computing in Python. *Nat Methods.* 2020;17:261–72. <https://doi.org/10.1038/s41592-019-0686-2>.
36. Gao F, Han L. Implementing the Nelder-Mead simplex algorithm with adaptive parameters. *Comput Optim Appl.* 2012;51(1):259–77. <https://doi.org/10.1007/s10589-010-9329-3>.
37. Storn R, Price K. Differential evolution – a simple and efficient heuristic for global optimization over continuous spaces. *J Glob Optim.* 1997;11(4):341–59. <https://doi.org/10.1023/A:1008202821328>.

38. Yaramyshev S, Barth W, Groening L, Kolomiets A, Tretyakova T. Development of the versatile multi-particle code DYNAMION. *Nucl Instrum Methods Phys Res, Sect A*. 2006;558(1):90–4. <https://doi.org/10.1016/j.nima.2005.11.018>.
39. Otani M. First Muon acceleration and muon linear accelerator for measuring the muon anomalous magnetic moment and electric dipole moment. *Prog Theor Exp Phys*. 2022;2022(5):052C01. <https://doi.org/10.1093/ptep/ptac067>. <https://academic.oup.com/ptep/article-pdf/2022/5/052C01/43753970/ptac067.pdf>.
40. Nakazawa Y, Cicek E, Futatsukawa K, Fuwa Y, Hayashizaki N et al. High-power test of an interdigital *h*-mode drift tube linac for the j-parc muon $g - 2$ and electric dipole moment experiment. *Phys Rev Accel Beams*. 2022;25:110101. <https://doi.org/10.1103/PhysRevAccelBeams.25.110101>.
41. Otani M, Mibe T, Yoshida M, Hasegawa K, Kondo Y et al. Interdigital H-mode drift-tube linac design with alternative phase focusing for Muon linac. *Phys Rev Accel Beams*. 2016;19(4):040101. <https://doi.org/10.1103/PhysRevAccelBeams.19.040101>.
42. Nakazawa Y, linuma H, Iwata Y, Iwashita Y, Otani M et al. Development of inter-digital H-mode drift-tube linac prototype with alternative phase focusing for a Muon linac in the J-PARC Muon G-2/EDM experiment. *J Phys Conf Ser*. 2019;1350:012054. <https://doi.org/10.1088/1742-6596/1350/1/012054>.
43. Li X, Pu Y, Yang F, Xie X, Gu Q et al. RF design and study of a 325 MHz 7 MeV APF IH-DTL for an injector of a proton medical accelerator. *Nucl Sci Tech*. 2019;30(9):135. <https://doi.org/10.1007/s41365-019-0657-4>.
44. Xie X, Pu Y, Yang F, Li X, Qiao J et al. Design of a 7-MeV APF DTL with robust considerations. *Nucl Instrum Methods Phys Res, Sect A*. 2018;908:49–59. <https://doi.org/10.1016/j.nima.2018.08.028>.
45. Xiucui X, Yuehu P, Zhentang Z. Cold test and beam commissioning of China's first homemade alternating-phase-focused drift tube linac. *High Power Laser Part Beams*. 2022;34(2022–0014):084007. <https://doi.org/10.11884/HPLPB202234.220014>.
46. Basten M, Aulenbacher K, Barth W, Burandt C, Dziuba F et al. Continuous wave interdigital *h*-mode cavities for alternating phase focusing heavy ion acceleration. *Rev Sci Instrum*. 2022;93(6):063303. <https://doi.org/10.1063/5.0094859>.
47. Hattori T, Matsui S, Hayashizaki N, Tomizawa H, Yoshida T et al. Compact IH-APF type linac for PIXE and RBS analyses. *Nucl Instrum Methods Phys Res B*. 2000;161:1174–7. [https://doi.org/10.1016/S0168-583X\(99\)00945-3](https://doi.org/10.1016/S0168-583X(99)00945-3).
48. Lu L, Hattori T, Hayashizaki N. Design and simulation of c^{6+} hybrid single cavity linac for cancer therapy with direct plasma injection scheme. *Nucl Instrum Methods Phys Res, Sect A*. 2012;688:11–21. <https://doi.org/10.1016/j.nima.2012.04.056>.
49. Lu L, Hattori T, Zhao H, Kawasaki K, Sun L et al. High power test of an injector linac for heavy ion cancer therapy facilities. *Phys Rev Spec Top, Accel Beams*. 2015;18:111002. <https://doi.org/10.1103/PhysRevSTAB.18.111002>.

Publisher's Note

Springer Nature remains neutral with regard to jurisdictional claims in published maps and institutional affiliations.

Submit your manuscript to a SpringerOpen[®] journal and benefit from:

- Convenient online submission
- Rigorous peer review
- Open access: articles freely available online
- High visibility within the field
- Retaining the copyright to your article

Submit your next manuscript at ► [springeropen.com](https://www.springeropen.com)
